

## Bistable Domain Wall Configuration in a Nanoscale Magnetic Disc: A Model for an Inhomogeneous Ferromagnetic Film

D. Venus\*

*Dept. of Physics and Astronomy, McMaster University, 1280 Main St. West, Hamilton Ontario, Canada*

(Received 18 August 2005)

Some polycrystalline ferromagnetic films are composed of continuously connected nanometer scale islands with random crystallite orientations. The nanometer perturbations of the film introduce a large number of nearly degenerate local field configurations that are indistinguishable on a macroscopic scale. As a first step, this situation is modelled as a thin ferromagnetic disc coupled by exchange and dipole interactions to a homogeneous ferromagnetic plane, where the disc and plane have different easy axes. The model is solved to find the partial Néel domain walls that minimize the magnetic energy. The two solutions give a bistable configuration that, for appropriate geometries, provides an important microscopic ferromagnetic degree of freedom for the film. These results are used to interpret recent measurements of exchange biased bilayer films.

**Key words :** Polycrystalline ferromagnetic film, Domain wall, Magnetic susceptibility, Activated dynamics, Interlayer exchange coupling

### 1. Introduction

The magnetic response of materials with a nanometer length scale - such as thin films, wires and particles - displays a wide range of phenomena of both fundamental and practical interest. In many cases, these systems can be understood qualitatively using homogeneous models where the material has one or two nanometer scale lengths; for instance, uniform thin films or wires. A more complicated case is where there are inhomogeneities or internal structure on the nanometer scale which give rise to magnetic phenomena.

As a recent example, consider a polycrystalline anti-ferromagnetic (AFM) film upon which a thin ferromagnetic (FM) film is deposited to form an exchange-biased system [1]. The columnar grains in the polycrystalline AFM have a cylinder radius of 3~20 nm, depending upon the fabrication procedure, and can have a very weak texture, or correlation, in their structural orientation from one grain to the next [2]. A thin magnetic film grown on top of this structure will have structural changes on the same scale, forming a collection of connected ferromagnetic islands with different crystal-

line orientations and local easy axes. The magnetic response of this type of system has been studied widely in order to understand the exchange coupling between the AFM and FM spins at the interface, and to investigate the resulting pinning of the FM by the AFM grains [3].

A recent study [4] of CoO/Co exchange-coupled bilayers using ac magnetic susceptibility, identified an important FM degree of freedom for this system with nanoscale heterogeneity. At low temperature the AFM configuration is frozen in by field-cooling so that the macroscopic FM magnetization is pinned through interfacial exchange. However, the polycrystalline growth of the FM islands results in a FM film with an easy axis that varies abruptly on the nanometer scale. This creates local field perturbations and introduces a large number of nearly degenerate field configurations which are indistinguishable on a macroscopic scale. A measurement of the transverse ac susceptibility reveals FM degrees of freedom that are activated at low temperature as the local magnetic configuration jumps between these nearly degenerate states. These low temperature FM degrees of freedom are effectively decoupled from the degrees of freedom of the AFM grains themselves, since the latter become activated at much higher temperature, near the Néel temperature. It is therefore permissible to analyse those FM and AFM degrees of freedom independently,

---

\*Corresponding author: Tel: +1-905-525-9140,  
Fax: +1-905-546-1252, e-mail: venus@physics.mcmaster.ca

and couple them weakly to describe the dynamics of the exchange biased system.

The present paper presents details of a simple model calculation of these FM degrees of freedom. It represents a FM island by a nanometer scale disc of thin film FM material with a given easy axis. The disc is coupled by FM exchange and long-range dipole interactions to the remainder of the film, that has a different easy axis. Two nearly degenerate domain wall configurations with an activation barrier between them create a local bistability. Under appropriate conditions, an applied ac field switches the system between these local states. A distribution of similar discs results in a broad dissipative peak in the imaginary component of the magnetic susceptibility at low temperature.

## 2. The Model

A schematic diagram of the model is given in Fig. 1a.

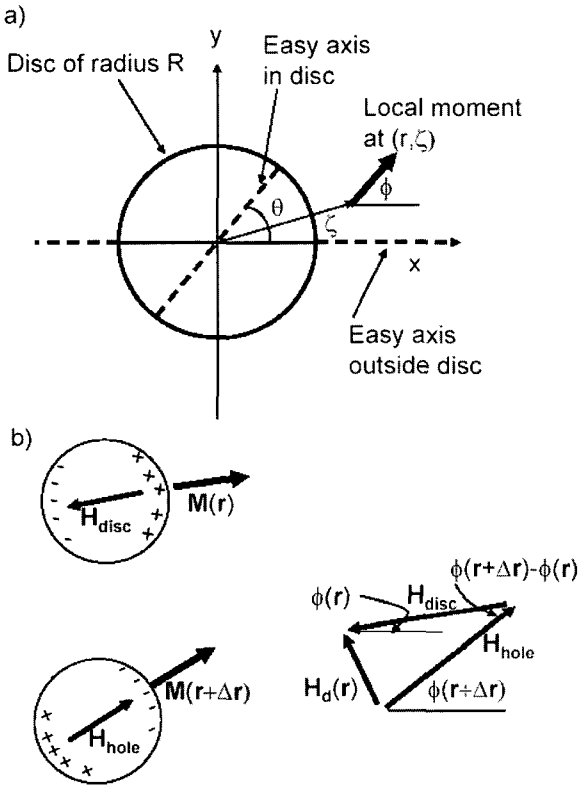


**Fig. 1.** a) An inhomogeneity in a thin film is modelled by a disc of radius  $R$  with an easy axis at angle  $\theta$  coupled to the rest of the plane, that has an easy axis along the  $x$  axis. The local moment at position  $(r, \zeta)$  is oriented at angle  $\phi$ . b) The demagnetization field for a ring of thickness  $\Delta r$  is the sum of the field due to disc of radius  $r$  and a hole of radius  $r + \Delta r$  in a magnetic plane.

The disc of radius  $R$  is centred on the  $xy$  axes, with the thickness  $t$  of the film perpendicular to the film. Inside the disc, the easy axis of magnetization is illustrated by the dashed line at angle  $\theta$  to the  $x$  axis. Outside of the disc, the film is considered to be uniform with an easy axis along the  $x$  axis. The large demagnetization energy accompanying any perpendicular component of magnetization in a thin film is supposed to restrict the magnetization to the  $xy$  plane. Since the film is much thinner than a magnetic domain wall, the variation of the magnetization through the film thickness is neglected. Therefore, the local moment orientation at each point  $(r, \zeta)$  in cylindrical co-ordinates is given by the angle  $\phi$ .

The simplest treatment of this model is to have different rigid moment directions inside and outside the disc. However, this is inappropriate because the nanometer scale disc is about the size or smaller than a domain wall width, and because it neglects the significant FM exchange energy at the boundary. It is necessary to use a continuum model and to find the domain wall configuration of lowest energy. Since demagnetization effects keep the magnetization within the plane, this will be a Néel wall [5] with a boundary condition at radius  $R$  and the constant magnitude of local magnetization  $M_S$ .

An important simplification arises by noting that the magnetic energy does not depend upon  $\zeta$ , and the magnetization direction is therefore determined by the function  $\phi(r)$ . This is because the problem has rotational symmetry, except for the easy axis directions. However, since the energy depends upon the easy axis direction only through  $\phi$  and not  $\zeta$ , there is nothing to break the rotational symmetry in  $\zeta$ . The anisotropy energy is

$$g[\phi(r)] = \begin{cases} K \sin^2(\theta - \phi(r)) & r < R \\ K \sin^2(\phi(r)) & r \geq R \end{cases} \quad (1)$$

An expression for the dipole energy can be derived from Fig. 1b. The demagnetization field created by a ring of magnetization from  $r$  to  $r + \Delta r$  in the plane is the sum of the field  $H_{hole}$  created by the entire magnetized plane at  $r' > r + \Delta r$  and the field  $H_{disc}$  created by the magnetized disc at  $r' < r$ . First consider  $H_{disc}$ . Since the orientation of the magnetization does not depend on  $\zeta$ ,  $M(r)$  is parallel at all points on the circumference of the disc. There is one point on the perimeter of the disc of radius  $r$  where  $M(r)$  is along the disc radius, as illustrated. This field geometry creates magnetic charges at radius  $r$  due the discontinuity of  $M$  that are equivalent to the well-known solution of the demagnetization field of a uniformly magnetized disc as approximated by a flat ellipsoid [6]. The corresponding

demagnetization field inside the disc,  $\mathbf{H}_{\text{disc}} = -N\mathbf{M}(\mathbf{r})$ . A similar argument holds for  $\mathbf{H}_{\text{hole}}$ , except because  $\phi$  changes between  $r$  and  $r + \Delta r$ , the demagnetization fields of the hole and disc are not parallel. They are added on the right of Fig. 1b to give the net demagnetization field due to the ring of radius  $r$  and thickness  $\Delta r$ :

$$H_d(r) = NM_s \frac{\partial \phi}{\partial r} \Delta r, \quad (2)$$

directed at an angle  $\phi(r) + \pi/2$  in the limit of small  $\Delta r$ .  $N$  is the in-plane demagnetization factor, and is expected to be small for the thin film. The magnetostatic energy due to the field from the ring is

$$dE_M(r) = -\frac{\mu_0}{2} \int_0^r d\mathbf{r}' \mathbf{M}(\mathbf{r}') \cdot \mathbf{H}_d(\mathbf{r}) \quad (3)$$

The total magnetostatic energy due to a sequence of such rings making up the xy plane is

$$E_M = \frac{\mu_0}{2} NM_s^2 \int_0^\infty dr \frac{\partial \phi}{\partial r} \int_0^r dr' \sin(\phi(\mathbf{r}) - \phi(\mathbf{r}')). \quad (4)$$

Using  $d\mathbf{r}' = 2\pi r' dr'$  and the boundary condition  $\phi(r \rightarrow \infty) \rightarrow 0$  gives the magnetostatic energy,

$$E_M = \frac{\mu_0}{2} NM_s^2 (2\pi t) \int_0^\infty dr r (1 - \cos[\phi(r)]). \quad (5)$$

The solution  $\phi(r)$  is found by minimizing the total energy [7]

$$E = 2\pi t \int dr r \left[ g(r) + h(r) + A \left( \frac{\partial \phi}{\partial r} \right)^2 \right], \quad (6)$$

With  $h(r) = (\mu_0/2) NM_s^2 (1 - \cos[\phi(r)])$ .  $A$  is the domain wall stiffness and is related to the FM exchange coupling energy per unit length. A variational procedure [7] gives the standard Euler equation  $g(\phi) + h(\phi) = A(\partial\phi/\partial r)^2$ , resulting in the solution

$$r(\phi) = \sqrt{A} \int_{\phi(0)}^{\phi(r)} \frac{d\phi}{\sqrt{g(\phi) + h(\phi)}}. \quad (7)$$

The minimized energy is

$$E = 4\pi t \sqrt{A} \int_{\phi_0}^{\phi_\infty} d\phi r(\phi) \sqrt{g(\phi) + h(\phi)}, \quad (8)$$

The notations used in the limits are  $\phi_0 \equiv \phi(r=0)$  and  $\phi_\infty \equiv \phi(r=\infty)$ .

### 3. Results

Calculations were performed for a Co film of thickness 8 nm, using bulk Co values for the anisotropy  $K = 5 \times$

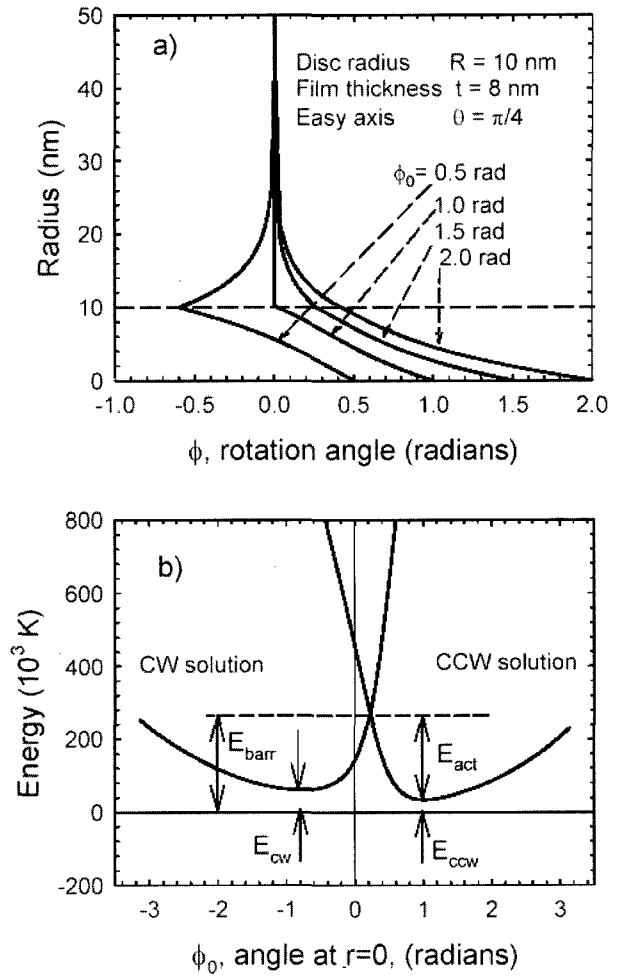


**Fig. 2.** a) Solutions for the partial domain wall configuration for different boundary conditions  $\phi_0$ . b) The total energy of the clockwise and counterclockwise partial domain wall solutions as a function of the boundary condition  $\phi_0$ . The energy minima  $E_{CCW}$  and  $E_{CW}$  are shown, as is the activation energy  $E_{act}$  between them.

$10^5$  J/m<sup>3</sup>, exchange stiffness  $A = 2.2 \times 10^{-11}$  J/m, and dipole constant  $(\mu_0/2)M_s^2 = 1.3 \times 10^6$  J/m<sup>3</sup>. Sample results for the radial variation of the magnetization,  $\phi(r)$  are shown in Fig. 2a for the specific case of a disc of radius  $R = 10$  nm with an easy axis at  $\theta = \pi/4$  from the x-axis. For the first-order equation in eq. (7), there is one arbitrary boundary condition,  $\phi_0$ , for which several values are assumed in the figure. The dashed horizontal line marks the disc radius. Note that a first-order differential equation also requires only continuity of value, and not of slope, at  $r = R$  where  $g[\phi(r)]$  is discontinuous [8]. It may appear that the exchange energy given in the continuum model by  $A(\partial\phi/\partial r)^2$  diverges here. However, the Heisenberg model from which it is derived shows no unphysical divergences so long as  $\phi(r)$  is continuous.

Therefore, no additional boundary term is needed in the expression for either  $\varphi(r)$  or the energy [9]. For  $r > R$  the moments rotate toward  $\varphi = 0$  since in this region both  $g(\varphi)$  and  $h(\varphi)$  approach zero at this angle and provide a boundary condition at infinity that ensures the system has a finite energy.

Fig. 2b gives the energy of the magnetic configuration as a function of the boundary condition  $\varphi_0$ . The CCW solution has  $0 > \theta > \pi/2$  and a minimum energy configuration  $E_{CCW}$ . The magnetization rotates to more positive values of  $\varphi$  as  $r$  decreases. The CW solution has a different minimum energy  $E_{CW}$ , since the easy axis is effectively at  $\theta_{CW} = \theta_{CCW} - \pi$ . Both have energy minima near the configuration that has  $\varphi(R) = 0$ , so that the entire partial domain wall is pushed inside the disc when  $R$  is relatively small. The value of  $\varphi_0$  that gives two solutions of the same energy defines an energy barrier  $E_{barr}$  that the system must pass over to move from one stable configuration to the other. The activation energy  $E_{act}$  for this FM degree of freedom is also marked on the figure.

Switching between these local energy minima occurs with a characteristic time,  $\tau$ , given roughly by [10]

$$\tau = \tau_0 \exp\left(\frac{E_a}{k_B T}\right), \quad (9)$$

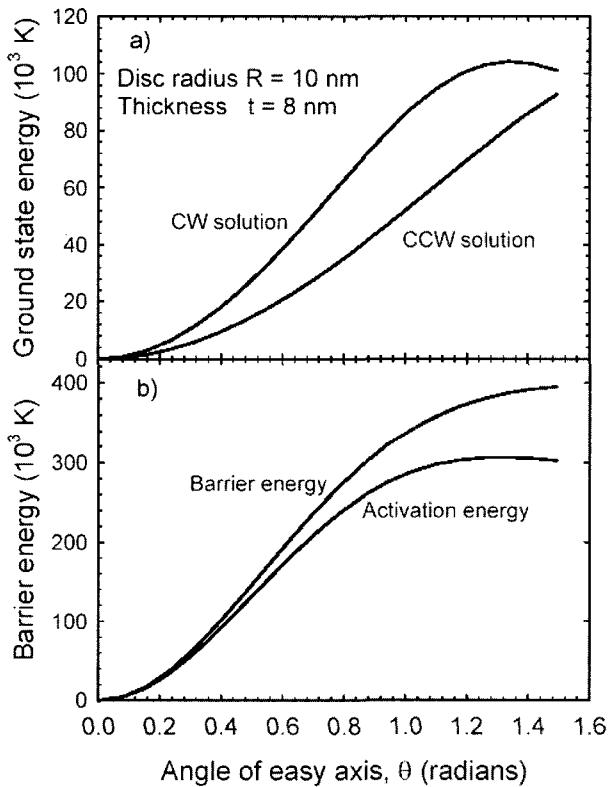


**Fig. 3.** The dependence of the energy minima and activation energy on the easy axis orientation of the disc, for a disc of radius 10 nm.

where  $\tau_0$  is typically  $10^{-9}$  s. Switching will be observed in the ac transverse susceptibility when  $\tau$  is of the order of the experimental time  $(2\pi\omega)^{-1}$ . For the parameters used in Fig. 2, and assuming an ac measurement frequency of 100 Hz, this will not occur until the temperature  $T \sim 1400$  K- that is, it will not be observed. However, a large range of activation energies is accessible in a collection of randomly oriented discs. Fig. 3 shows calculations for the two minimum energy configurations, and for the activation energy between them, as a function of the easy axis angle,  $\theta$ , for a disc of the same radius  $R = 10$  nm. Fig. 4 shows similar calculations as a function of disc radius, for a fixed easy axis at  $\theta = \pi/4$ . It is apparent that for smaller disc radii of 3 to 7 nm, and for all disc sizes when the easy axis is close to the x axis, that the activation energies of  $\sim 10^3$  K corresponding to switching at  $\sim 50$  K can be easily obtained.

These results can be used to understand quantitatively the ac susceptibility of CoO/Co bilayers [4], where the islands sizes are 3 to 7 nm, depending upon the CoO thickness [2]. There are two classes of FM islands: those with a low-temperature, thermally activated, local FM degree of freedom; and those that are not thermally activated before the system reaches the blocking temperature. This

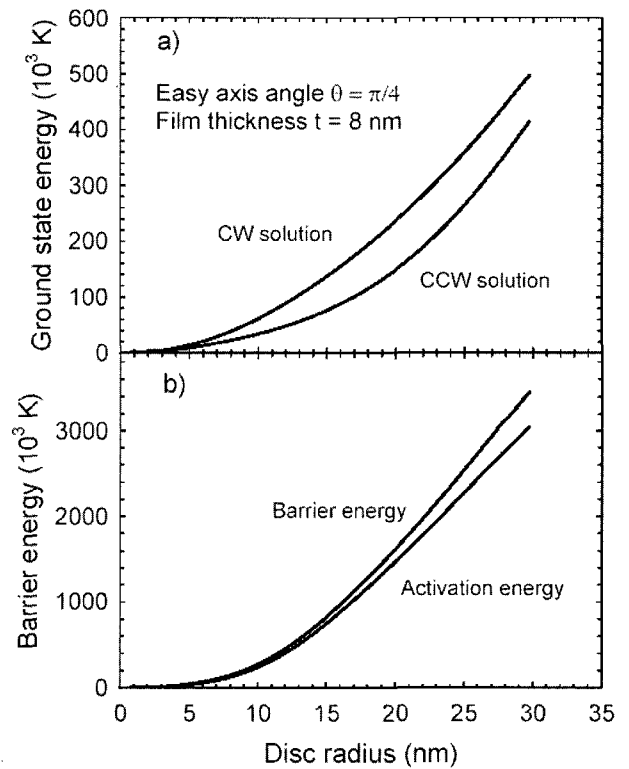


**Fig. 4.** The dependence of the energy minima and activation energy on the radius of the disc, for a disc with an easy axis oriented at  $\theta = \pi/4$ .

gives rise to the two distinct peaks in the imaginary component of the ac susceptibility, as discussed in ref. (4). The high energy peak is well understood as the dissipation associated with the “unblocking” of the FM due to the thermal activation of the AFM grains just below the Néel temperature of the AFM [11]. The low temperature peak is due to the thermal activation of the domain wall bistability of FM islands with low activation energies. In the presence of an ac field, these islands are no longer effectively pinned by the AFM. This causes a dramatic reduction in the interfacial exchange anisotropy field measured using ac susceptibility as the sample is heated from 4 K to about 70 K. Large field measurement of the same anisotropy field (exchange biased hysteresis loops) are not sensitive to the smaller scale energies of the domain wall instability of the islands, so the low temperature variation of the exchange field is not seen [12]. This is the root of the difference of a factor of 2 or 3 in the exchange bias field as measured by low field and high field methods [13].

### References

- [1] W. H. Meiklejohn and C. P. Bean, Phys. Rev. **102**, 1413 (1956).
- [2] Y. J. Tang, D. J. Smith, B. L. Zink, F. Hellman, and A. E. Berkowitz, Phys. Rev. B **67**, 054408, (2003).
- [3] K. Takano, R. H. Kodama, A. E. Berkowitz, W. Cao, and G. Thomas, Phys. Rev. Lett. **79**, 1130 (1997).
- [4] D. Venus and F. Hunte, Phys. Rev. B **72**, 024404 (2005).
- [5] L. Néel in *Selected Works of Louis Néel*, ed. N. Kurti (Gordan and Breach, New York, 1988), p. 232.
- [6] S. Chikazumi, *Physics of Ferromagnetism* (Clarendon, Oxford, 1997) ch. 1.
- [7] S. Chikazumi, *Physics of Ferromagnetism* (Clarendon, Oxford, 1997) ch. 16.
- [8] This is very different than for the problem of a planar boundary between two half-infinite film with different directions of the easy axis. In that case, reflection symmetry imposes the additional requirement of a continuous derivative across the boundary. See ref. 7.
- [9] This would not be the case in a rigid moment model, where  $\varphi(r)$  is discontinuous at  $r = R$ .
- [10] W. F. Brown, Phys. Rev. **130**, 1677 (1963).
- [11] E. Fulcomer and S. H. Charap, J. Appl. Phys. **43**, 4184 (1972).
- [12] T. Gredig, I. N. Krivorotov, and E. Dan Dahlberg, J. Appl. Phys. **91**, 7760 (2002). These measurements use hysteresis loops and study the same samples as in ref. 4.
- [13] H. Xi and R. M. White, J. Appl. Phys. **87**, 4960 (2000); J. Geshev, Phys. Rev. B **62**, 5627 (2000).